

Comparisons of SHM Sensor Models with Empirical Test Data for Sandwich Composite Structures

V. HAFIYCHUK, D. G. LUCHINSKY, V. N. SMELYANSKIY,
R. TYSON, J. MILLER and C. BANKS

ABSTRACT

This paper reports on analytical work, as well as experimental testing, that were accomplished at the Ames Research Center and at the Marshall Space Flight Center to examine acoustic wave propagating and the ability to detect intrinsic faults in sandwich type composite structures. Sandwich type composites are being studied for use in NASAs new heavy lift launch vehicle and flaw detection is crucial for safety and for failure prognostics. The work reported on in this paper involved both the theoretical modeling as well as comparison with empirical testing needed to answer the question of feasibility for reliable, and accurate, structural health monitoring (SHM) in the composite structure of interest. The analytical model of the transient wave propagation and scattering based on the Mindlin plate theory was developed. A scattered transient field properties are calculated theoretically using this model and numerically using the finite element model for acoustic waves generated by an acoustic-patch actuator. It is shown that theoretical results are in agreement with the results of numerical simulations and with experimental results.

Introduction

Composite sandwich panels (CSP) are replacing metals in engineering applications due to their high strength and low weight properties, as well as their flexible production capabilities [1]. Their stiffness-to-weight ratios and the lack of corrosion lead to the wide usage of them in the naval ships, airplanes, bodies for vehicles and trains, etc. They are very prospective for space applications where light flight structures immediately lead to higher payloads. CSP, to which we restrict our consideration here, are complex structural materials made from stiff facesheets and soft cores and are usually referred to as sandwiches with soft cores. Sandwich panels have one basic drawback in common: they all share failure mechanisms and structural failures occur internally, out of the view of normal visual means of inspection. Internal de-bonds, de-laminations, cracks, and/or buckles are

V. Hafiychuk, D. G. Luchinsky and V. N. Smelyanskiy, NASA Ames Research Center, Mail Stop 269-3, Moffett Field, CA 94035, USA

R. Tyson, University of Alabama, 1804 Sparkman Dr. Huntsville, AL 35816, USA

J. Miller and C. Banks, NASA Marshall Space Flight Center, Huntsville, AL 35812

Report Documentation Page

Form Approved
OMB No. 0704-0188

Public reporting burden for the collection of information is estimated to average 1 hour per response, including the time for reviewing instructions, searching existing data sources, gathering and maintaining the data needed, and completing and reviewing the collection of information. Send comments regarding this burden estimate or any other aspect of this collection of information, including suggestions for reducing this burden, to Washington Headquarters Services, Directorate for Information Operations and Reports, 1215 Jefferson Davis Highway, Suite 1204, Arlington VA 22202-4302. Respondents should be aware that notwithstanding any other provision of law, no person shall be subject to a penalty for failing to comply with a collection of information if it does not display a currently valid OMB control number.

1. REPORT DATE SEP 2011	2. REPORT TYPE N/A	3. DATES COVERED -	
4. TITLE AND SUBTITLE Comparisons of SHM Sensor Models with Empirical Test Data for Sandwich Composite Structures		5a. CONTRACT NUMBER	
		5b. GRANT NUMBER	
		5c. PROGRAM ELEMENT NUMBER	
6. AUTHOR(S)		5d. PROJECT NUMBER	
		5e. TASK NUMBER	
		5f. WORK UNIT NUMBER	
7. PERFORMING ORGANIZATION NAME(S) AND ADDRESS(ES) NASA Ames Research Center, Mail Stop 269-3, Moffett Field, CA 94035, USA		8. PERFORMING ORGANIZATION REPORT NUMBER	
9. SPONSORING/MONITORING AGENCY NAME(S) AND ADDRESS(ES)		10. SPONSOR/MONITOR'S ACRONYM(S)	
		11. SPONSOR/MONITOR'S REPORT NUMBER(S)	
12. DISTRIBUTION/AVAILABILITY STATEMENT Approved for public release, distribution unlimited			
13. SUPPLEMENTARY NOTES See also ADA580921. International Workshop on Structural Health Monitoring: From Condition-based Maintenance to Autonomous Structures. Held in Stanford, California on September 13-15, 2011 . U.S. Government or Federal Purpose Rights License.			
14. ABSTRACT This paper reports on analytical work, as well as experimental testing, that were accomplished at the Ames Research Center and at the Marshall Space Flight Center to examine acoustic wave propagating and the ability to detect intrinsic faults in sandwich type composite structures. Sandwich type composites are being studied for use in NASAs new heavy lift launch vehicle and flaw detection is crucial for safety and for failure prognostics. The work reported on in this paper involved both the theoretical modeling as well as comparison with empirical testing needed to answer the question of feasibility for reliable, and accurate, structural health monitoring (SHM) in the composite structure of interest. The analytical model of the transient wave propagation and scattering based on the Mindlin plate theory was developed. A scattered transient field properties are calculated theoretically using this model and numerically using the finite element model for acoustic waves generated by an acoustic-patch actuator. It is shown that theoretical results are in agreement with the results of numerical simulations and with experimental results.			
15. SUBJECT TERMS			
16. SECURITY CLASSIFICATION OF:			17. LIMITATION OF ABSTRACT
a. REPORT unclassified	b. ABSTRACT unclassified	c. THIS PAGE unclassified	SAR
			18. NUMBER OF PAGES 8
			19a. NAME OF RESPONSIBLE PERSON

typical local failure modes, decrease the strength of composite material sandwich structures, and may lead to serious damages and even to structure disintegration.

Many methods are used for investigating acoustic wave propagation and scattering in the framework of structural health monitoring (SHM). We consider that the waves are excited by piezoelectric transducers (PZT), which act both as actuators and sensors. In this paper we use plate theory for analytical investigation of wave propagation in sandwich panels, discuss parameters, governing equations, and the properties of the basic sandwich panel. High-fidelity simulations are employed to compare the results of the simulation with analytical results. Some comparison with experimental study is made.

Plate theory for sandwich structures.

In a Mindlin plate theory the displacements of the plate in the transverse, radial, and tangential direction components are expressed as follows [2-5]

$$w = w(r, \theta, t), u = z\psi_r(r, \theta, t), v = z\psi_\theta(r, \theta, t),$$

where z is the coordinate defining points across the thickness of the plate ($z = 0$ is the neutral plane) and w is the out-of-plane displacement, ψ_r and ψ_θ are the rotations of vertical lines perpendicular to the mid-plane. The governing equations for the symmetric honeycomb panels in terms of moments M and shear forces Q can be presented as

$$\frac{1}{r} \frac{\partial Q_\theta}{\partial \theta} + \frac{\partial}{\partial r} Q_r + \frac{1}{r} Q_r - Q_\theta = \rho \frac{\partial^2}{\partial t^2} w, \quad (1)$$

$$\frac{\partial M_{rr}}{\partial r} + \frac{1}{r} M_{rr} - \frac{1}{r} M_{\theta\theta} + \frac{1}{r} \frac{\partial}{\partial \theta} M_{r\theta} - Q_r = I \frac{\partial^2}{\partial t^2} \psi_r, \quad (2)$$

$$\frac{1}{r} \frac{\partial M_{r\theta}}{\partial r} + \frac{2}{r} M_{r\theta} + \frac{1}{r} \frac{\partial}{\partial \theta} M_{\theta\theta} - Q_\theta = I \frac{\partial^2}{\partial t^2} \psi_\theta, \quad (3)$$

where $\rho = \sum_{k=1}^3 \int_{a_k}^{b_k} \rho_k dz$, is the mass density per unit area of the plate, index k corresponds to the material layer, ρ_k is the density, $I = \sum_{k=1}^3 \int_{a_k}^{b_k} \rho_k z^2 dz$ is the mass moment of inertia. Each layer in the sandwich panel is bounded by the coordinates a_k and b_k in the thickness direction as shown in the Fig. 1. The stress resultants in terms of moments M_{rr} , $M_{\theta\theta}$, and $M_{r\theta}$, along with shear forces Q_r and Q_θ can be related to the transverse displacements and rotations as follows:

$$M_{rr} = \frac{D}{r} \left[r \frac{\partial \psi_r}{\partial r} + \nu (\psi_r + \frac{\partial \psi_\theta}{\partial \theta}) \right], M_{r\theta} = \frac{D(1-\nu)}{2r} \left[\frac{\partial \psi_r}{\partial \theta} - \psi_\theta + r \frac{\partial \psi_\theta}{\partial r} \right], \quad (4)$$

$$M_{\theta\theta} = \frac{D}{r} \left[\nu r \frac{\partial \psi_r}{\partial r} + \psi_r + \frac{\partial \psi_\theta}{\partial \theta} \right], Q_r = 2G \left(\psi_r + \frac{\partial}{\partial r} w \right), Q_\theta = 2G \left(\psi_\theta + \frac{1}{r} \frac{\partial}{\partial \theta} w \right),$$

where $D = E_f t_f^3 / 6 + E_c t_c^3 / 12 + E_f t_f (t_f + t_c)^2 / 4$ - is the flexural stiffness, ν is the Poisson ratio, which for the sake of simplicity is taken as equal for each layer, E_f , E_c

- Young's modulus of the facesheet and the core, correspondingly, t_f , t_c - thicknesses of the facesheet and the core layers, G is the shear stiffness of the plate.

Wave propagation. The general solution of the acoustic waves propagation with cycling frequency ω is $(w, \psi) = Re[(W, \Psi) \exp(-i\omega t)]$ [2-7], where and throughout this paper, $Re(\cdot)$ denotes the real part of the quantity in parentheses, $\psi = (\psi_r, \psi_\theta)$. For isotropic sandwich layers wavenumbers have three brunches:

$$k_{1,2}^2 = (k_p^2 + k_s^2) / 2 \pm \sqrt{k_f^4 + (k_p^2 - k_s^2)^2 / 4}, \quad k_3^2 = k_1^2 k_2^2 / k_p^2, \quad (5)$$

where

$$k_s = \omega / c_s, k_p = \omega / c_p, k_f = (\rho \omega^2 / D)^{1/4}, c_s = (G / \rho)^{1/2}, c_p = (D / I)^{1/2}.$$

The flexural wave corresponds to the real ω, k in whole ω domain. The second (and third) dilatation branch of (k, ω) dependence become real starting from the cutoff frequency.

Model of the scatterer. The scattering problem for Mindlin plate theory was considered in several articles. Pao and Chao [6] considered scattering of a flexural wave at a circular hole. The circular inhomogeneity was considered in [4] and the graduate damaged model - in [7].

Let us consider the following scattering problem (see Fig. 1b). The circular delamination (debond) is located at the center of the sandwich composite panel ($x=y=0$). The source of the cylindrical wave generated by PZT sensor is located at a distance b from the center of the circular delamination ($x=-b, y=0$). In this paper we extend the damage model of the defect in the CSPs in such a way that it allows us to differentiate between the delamination and debonding faults. The sketch of the damage model is shown in Fig. 1a. It consists of two vertically stack circular cylinders with integral properties depending on the location of the fault. If the fault is located in the facesheet the model represents a delamination. If the fault is located at the interface between the facesheet and the soft core the model represents a debond. To find the parameters of the fault we will use formulas for a non-symmetrical sandwich panel [1], which for brevity are not presented here. In this case, the symmetrical sandwich part of the panel is denoted by index 1. The delaminated region consists of two subregions (see Fig. 1b): (i) a subregion with the sandwich core denoted by index 2 and (ii) the delaminated facesheet subregion denoted by index 3 with plate parameters D_2, I_2, G_2, ρ_2 and D_3, I_3, G_3, ρ_3 , correspondingly. If we introduce wavenumbers k_{ij} for the delaminated regions we can use the dispersion relation for the roots (5) with parameters corresponding to indices 2 and 3 (index 1 belongs to the symmetric sandwich panel without any damage). As a result, we get a square matrix of k_{ij} where the first index is a number of a root (5) and the second one is a number of a media ($j=1,2,3$). For the self-consistent behavior of the delaminated region we impose boundary conditions between the delaminated region and the healthy annular sandwich beam. These conditions include the continuity of the plate displacements, the equality of the slopes, moments and shear forces at $r=a$:

$$\begin{aligned} w^1 = w^2 = w^3, \quad \psi_r^1 = \psi_r^2 = \psi_r^3, \quad \psi_\theta^1 = \psi_\theta^2 = \psi_\theta^3, \\ M_{rr}^1 = M_{rr}^2 + M_{rr}^3, \quad M_{r\theta}^1 = M_{r\theta}^2 + M_{r\theta}^3, \quad Q_r^1 = Q_r^2 + Q_r^3, \end{aligned} \quad (6)$$

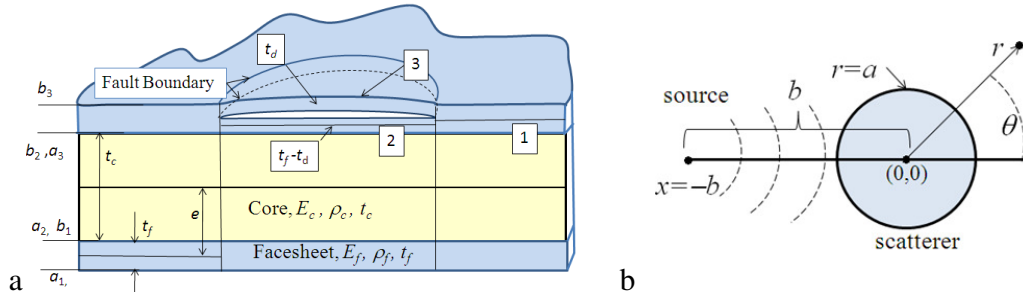


Figure 1. Sketch of the sandwich structure with delamination fault. Domain 1 (healthy panel) is connected with two domains 2 and 3 through the boundary of the fault – a, Geometry of the scattering of the incident wave - b .

where moments and shear forces are described by expressions (4), with corresponding indices.

Incident wave. We will consider a circular-patch actuator on the Mindlin plate generated by a surface traction plate waves in the form derived in [2,5]. For the sake of brevity let us consider only w^{in} component which for the actuation circular force leads to the incident wave for $r < b$

$$w^{in}(r, \omega) = \sum_{n=0, i=1}^{\infty, 2} s_i \varepsilon_n (-1)^n H_n(k_{i1}b) J_n(k_{i1}r) \cos(n\theta), \quad (7)$$

where s_i are a certain constants depending on wavenumbers k_i and Hankel functions $H_0(k|r+b|)$ are expanded into a Fourier series and ε_n is the Neumann factor, $\varepsilon_0=1$, $\varepsilon_n=2$ ($n=1,2,3,\dots$) [8].

The solution of scattering waves from the fault. If we consider that equations (1)-(4) are true for each domain: outside the damage and inside of it ($j=1,2,3$), the solution is separated into three domains, where the delaminated region, in turn, consists of two domains. As a result, the general solution can be represented for $r > a$ by incident and scattered waves. We seek the solution in the form of a linear combination of the scattered and incident waves. The functions we have used for the solution should be finite at $r=0$ and vanish at $r \rightarrow \infty$. As a result, the general solution for the domains $i = 1,2,3$ is

$$w(r, t, \theta) = \text{Re} \sum_{n=0}^{\infty} e^{-i\omega t} \cos(n\theta) \begin{cases} w^1 \equiv w_n^{in} + a_{1n} H_n(k_{11}r) + a_{2n} H_n(k_{21}r) |_{r>a} \\ w^2 \equiv a_{4n} J_n(k_{12}r) + a_{5n} J_n(k_{22}r) |_{r \leq a} \\ w^3 \equiv a'_{4n} J_n(k_{13}r) + a'_{5n} J_n(k_{23}r) |_{r \leq a} \end{cases} \quad (8)$$

Here wavenumbers k_{ij} are calculated for three media and the first index i corresponds to a root, and the second index j - to a medium (expressions for ψ_r, ψ_θ are not presentet here for making writing concise). The boundary conditions (6), lead to a system of linear algebraic equations for each value of n

$$A_n u_n = b_n \quad (9)$$

The matrix A_n and vector b_n and complete list of the matrix elements can be calculated by symbolic calculus and is not presented here.

As a result we obtain a system of linear algebraic equations relative to

constants $u_n = (a_{1n}, a_{2n}, a_{3n}, a_{4n}, a'_{4n}, a_{5n}, a'_{5n}, a_{6n}, a'_{6n})^T$, which can be solved numerically. We find that the first several main modes determine the spectrum of the scattered wave, and truncation of n at $n=30-50$ in equations (9) gives practically the same result at any desired wave frequencies. According to the expression of a_{1n} , a_{2n} :

$$a_{1n}(\omega) = \frac{\det A_{1n}(k_{ij}(\omega)a)}{\det A_n(k_{ij}(\omega)a)}, \quad a_{2n}(\omega) = \frac{\det A_{2n}(k_{ij}(\omega)a)}{\det A_n(k_{ij}(\omega)a)}, \quad (10)$$

the elastic field around the circular debond is computed and the coefficients a_{1n}, a_{2n} determine displacements outside the debond region. In expressions (10) matrix $A_{1n}(k_{ij}a)$ is obtained by substituting the first column in matrix $A_n(k_{ij}a)$ by the left hand side column, and matrix $A_{2n}(k_{ij}a)$ - by substituting the second column by the right hand side column. As a result, for out of plane solution for $r > a$, the formula can be presented as

$$w(r, \theta, \omega) = \text{Re} \sum_{n=0}^{\infty} \cos(n\theta) [w_n^{in}(r) + a_{1n}(\omega)H_n(k_{11}(\omega)r) + a_{2n}(\omega)H_n(k_{21}(\omega)r)] e^{-i\omega t} \quad (11)$$

The first term in (11) corresponds to the incident wave, second - to the flexural mode with a wavenumber k_{11} and the third one describes the flexural wave with a wavenumber k_{21} propagating above the cutoff frequency. Below the cutoff frequency ($\omega < \omega_c$) the third term corresponds to the evencent wave. The solution for rotations of vertical lines perpendicular to the mid-plane ψ_r and ψ_θ can be determined in a similar way.

Transient Solution. To study the transient wave propagation we consider that the plate is excited by a pulse of the load stimulated by a PZT sensor. The expression for the wave pulses in the plane (x,y) may be derived from the steady-state solution in the frequency domain by applying the Fourier transform technique. For the Fourier spectrum $G(\omega)$ of the signal $g(t)$ the final solution for out of plane field outside the debond in the time domain will be

$$w(r, \theta, t) = \text{Re} \frac{1}{2\pi} \int_{-\infty}^{\infty} G(\omega) w(\omega, r, \theta) e^{-i\omega t} d\omega \quad (12)$$

We consider the Hanning type actuation signals which are usually used for fault detection in SHM. Out of plane displacement (8) is an analytical solution of

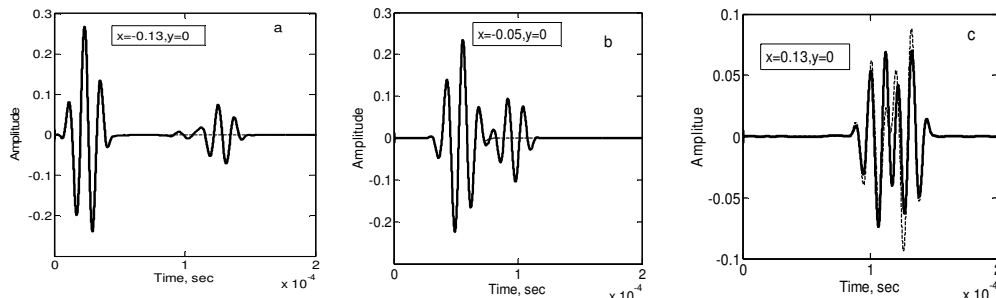


Figure 2. Wave propagation and scattering by the debond region located at the center of the plate (dashed line – pristine plate, solid black line – plate with delamination: $x=-13.5\text{cm}$ – a), $x=-5\text{cm}$ – b), $x=13\text{cm}$ – d).

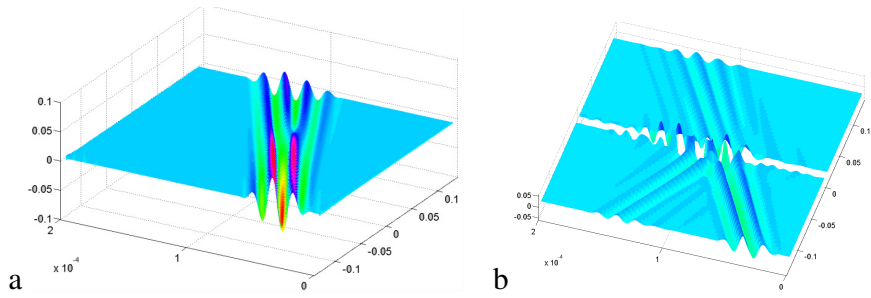


Figure 3. Wave propagation without a debond presented in coordinates (x,t) along the line $y=0$. No scattering domain – a); Scattering from the debond region located at the center. Path is taken along the line passing through the centers of the source and the scatterer – b).

the scattering problem and makes it possible to investigate the transient pulse propagation, and to compare the obtained results with the finite element simulation.

In Fig. 2 the transient pulse propagation determined by formulas (8),(12) is presented for different points of the line passing through the actuator and the fault. The dynamics of the propagating signal for pristine plate for these points of the structure is plotted by the blue dashed line and the w displacement of the debond plate is depicted by the black line. We can see that for the pristine plate without a fault, the wave propagates without any reflection and due to the dispersion we have an increasing number of oscillations (Fig. 3 a). In the plate with a fault we see that after scattering the propagating signal partially propagates back and continues to propagate forward in the initial direction (Fig. 3 b). The transient solution of the propagating wave as a result of calculation of the expression (7) shows that the form of the signal is different for each specific point of the plate. While analyzing the structure of the transient signal we can see two main features. The signal for the points located sufficiently far from the fault consists of the direct signal and the reflected one of the similar form propagating back. Signals passing along the straight line connecting the actuator with the fault have counter motion as it is seen from Figures 2 and 3. The measurement of the back-propagating signal, which can be detected by the pulsed echo technique, and the forward-propagating one detected by the pitch-catch method, can retrieve information about the fault since they carry this information while propagating through the plate.

When transient waves are used to detect delamination in the sandwich plate, the total solution can be written as a superposition of the incident and scattering waves in the time domain containing $n + 1$ different modes (7).

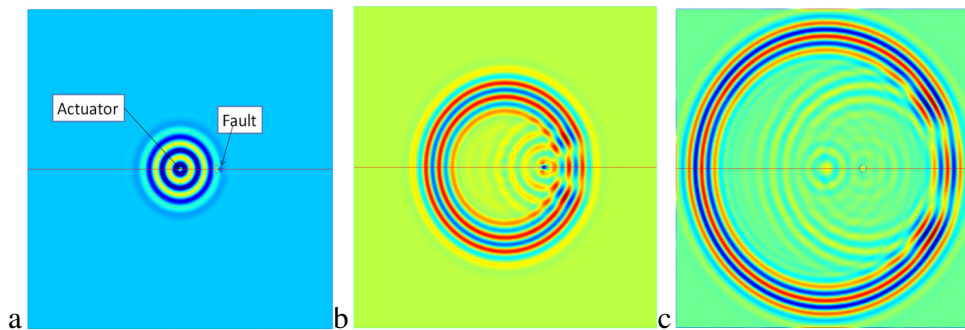


Figure 4. FE modeling of wave propagation from the center and scattering from the debond region (view in x,y plane, damage is located at $x=14\text{cm}$ from the center $(0,0)$ at $t=0.45 \times 10^{-4}\text{s}$ – a), $t=0.9 \times 10^{-4}\text{s}$ – b, $t=1.35 \times 10^{-4}\text{s}$ – c).

We compare the analytical results with the corresponding results obtained by the Finite Element simulation. The FE modeling for 2D Mindlin plate is presented in Fig. 4. and it fits well with the theoretical approach. The main difference between these signals is that the theoretical results are valid for the infinite plate, and the FE 2D Mindlin plate model gives the result which takes into account reflections from the boundaries. The comparison of the 3D modeling of sandwich composite panels with the theoretical result is considered in the last section. The propagation of the wave originated at the center of the plate (0,0) and scattered from the debond region located at the distance $b=0.14\text{m}$ apart is presented in Figure 4. You can see that the cylindrical out-of- plane wave propagates without any reflections (Figure 4 a), and the scattered from the debond region wave excites the vibration of the debond generating a pulsed echo signal and a changing pitch catch signal.

Experimental, Analytical and FE comparisons. An experiment in Lamb wave propagation in a honeycomb sandwich panel was done by Metis Design Inc. in collaboration with ARC NASA. The sandwich panel fabricated for this test consisted of two 84-mil thick cross-ply carbon fiber composite laminates (bonded to a 1"- thick aluminum honeycomb core). The size of the panel was $1\text{ft}\times 1\text{ft}$. In the experiment, PZT sensors located on the facesheet of the honeycomb panel were used to determine the deformation at a different location (See disks located on the panel which correspond to real PZT sensors in the experiment). The results of the comparison voltage on these PZT sensors are presented in Figure 5 b, c.

The obtained experimental time domain results are compared with the corresponding results of the FE simulations in Abaqus. The FE analysis makes it possible to find the amplitude of all displacements (u, v, w) in 3D simulations as well as the stresses and strains under an external excitation depending on the frequency of the excitation. The FE model was built as an exact copy of the experimental panel. It was meshed to define the solution's resolution and satisfy the tolerance conditions, which make it possible to investigate the acoustic wave propagation through a layered sandwich plate. The discretization was chosen to determine the wavelength with a high resolution at several elements per wavelength limits. Finite element 3D modeling of real honeycomb structure with laminate facesheets is performed in order to validate the approximating Mindlin plate theory analytical approaches and to get more realistic results in application of the homogenized structure model for SHM. The finite element simulation of Abaqus Explicit has

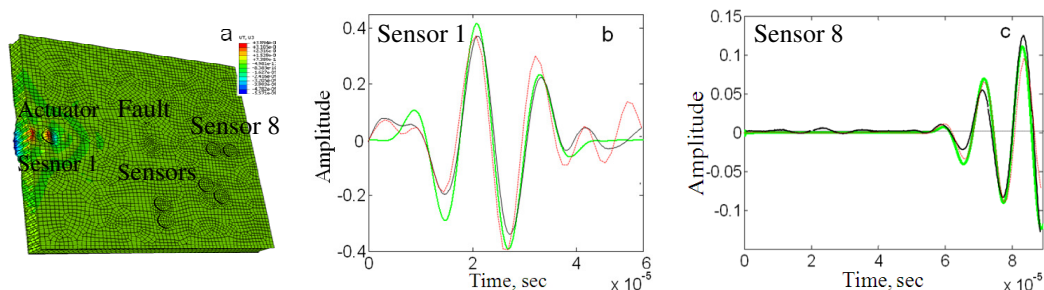


Figure 5. View of the panel FE model used for experimental investigation of wave propagation and scattering – a); Sensor signal in mV on the sensors located at a distance of 25cm apart from each other for a sandwich composite panel: $x=-12.5\text{cm}$ – b and $x=12.5\text{cm}$ – c. The red line – experimental data, black line – FE simulations and the green line – fitted Mindlin plate theory results.

been used to determine the PZT actuation of the sandwich plate. The small debond fault was introduced at the center of the plate (Fig. 5 a). For the sandwich structure we performed the simulation of the several possible layups we come across in developing SHM methods. The actuator and the sensor were simulated as PZT discs (14mm and 7mm in diameter and 2mm in thickness). The excitation source was positioned at a distance b from the damaged area and the receiving sensors are located in (x, y) plane as it is seen from the plots.

In the Mindlin plate theory we do not consider coupling with piezo sensors and that is why we cannot plot a real electric signal on this plot. We used comparing relative amplitude and phase velocity to show how the Mindlin plate theory results relate to a real structure. The comparison of out of plane displacement dynamics shows that the obtained results are a sufficiently good fit to analytical results. The simulations are done for modeled structures with 1in core and 84mil face sheets in thickness.

It should be mentioned that the results of modeling wave propagation and scattering in sandwich composite plates fit well to the theoretical ones only for small time intervals. For a longer time interval, the experimental result differs significantly from the theoretical approach. However, if in the case of FE modeling we can fit experimental and numerical signals for a longer time, here the theoretical approach is proposed for the infinite plate only.

Conclusion

This paper addresses the simulation of the guided wave propagation and scattering in sandwich structures with the emphasis given to the properties which can be used for SHM. The analytical investigation of the plate wave using the Mindlin plate theory and the numerical simulations shows the main features we come across when developing real SHM methods. An analytical study is carried out to find the solution for transient wave propagation and scattering from the delaminated and the debond area. The obtained analytical solutions are compared to the FE analysis as well as the experimental data.

REFERENCES

1. D. Zenkert, Ed. The Handbook of Sandwich Construction, EMAS Ltd, Warley, UK (1997).
2. R. F. Rose and C. H. Wang. "Mindlin plate theory for damage detection: Source solutions". *J. Acoust. Soc. Am.* 116 (1), 154-171 (2004).
3. S.D. Yu, W.L. Cleghorn. "Free flexural vibration analysis of symmetric honeycomb panels" *Journal of Sound and Vibration* 284, 189—204 (2005).
4. C. Vemula and A. N. Norris. "Flexural wave propagation and scattering on thin plates using Mindlin theory", *Wave Motion* 26, 1-12 (1997).
5. C. H Wang, J. T Rose and F.K. Chang. "A synthetic time-reversal imaging method for structural health monitoring". *Smart Mater. Struct.* 13, 415-423 (2004).
6. Y-H Pao, CC Chao, "Diffractions of flexural waves by a cavity in an elastic plate", *AIAA J* 2(11), 2004-2010 (1964).
7. C. H. Wang, Fu-Kuo Chang. "Scattering of plate waves by a cylindrical inhomogeneity". *Journal of Sound and Vibration* 282, 429-451 (2005).
8. P.M. Morse, H. Feshbach. *Methods of Theoretical Physics*, McGraw-Hill, New York (1953).